

BET Bromodomain Inhibition Blocks an AR-Repressed, E2F1-Activated Treatment-Emergent Neuroendocrine Prostate Cancer Lineage Plasticity Program



Dae-Hwan Kim¹, Duanchen Sun¹, William K. Storck^{2,3}, Katherine Welker Leng^{2,3}, Chelsea Jenkins¹, Daniel J. Coleman¹, David Sampson¹, Xiangnan Guan¹, Anbarasu Kumaraswamy^{2,3}, Eva S. Rodansky^{2,3}, Joshua A. Urrutia¹, Jacob A. Schwartzman¹, Chao Zhang^{2,3}, Himisha Beltran⁴, Mark P. Labrecque⁵, Colm Morrissey⁵, Jared M. Lucas⁶, Ilsa M. Coleman⁶, Peter S. Nelson⁶, Eva Corey⁵, Samuel K. Handelman⁷, Jonathan Z. Sexton⁷, Rahul Aggarwal⁸, Wassim Abida⁹, Felix Y. Feng⁸, Eric J. Small⁸, Daniel E. Spratt^{3,10}, Armand Bankhead III^{3,11,12}, Arvind Rao^{3,11,13}, Emily M. Gesner¹⁴, Sarah Attwell¹⁴, Sanjay Lakhota¹⁴, Eric Campeau¹⁴, Joel A. Yates^{2,3}, Zheng Xia¹, and Joshi J. Alumkal^{1,2,3}

ABSTRACT

Purpose: Lineage plasticity in prostate cancer—most commonly exemplified by loss of androgen receptor (AR) signaling and a switch from a luminal to alternate differentiation program—is now recognized as a treatment resistance mechanism. Lineage plasticity is a spectrum, but neuroendocrine prostate cancer (NEPC) is the most virulent example. Currently, there are limited treatments for NEPC. Moreover, the incidence of treatment-emergent NEPC (t-NEPC) is increasing in the era of novel AR inhibitors. In contrast to *de novo* NEPC, t-NEPC tumors often express the AR, but AR's functional role in t-NEPC is unknown. Furthermore, targetable factors that promote t-NEPC lineage plasticity are also unclear.

Experimental Design: Using an integrative systems biology approach, we investigated enzalutamide-resistant t-NEPC cell lines and their parental, enzalutamide-sensitive adenocarcinoma cell

lines. The AR is still expressed in these t-NEPC cells, enabling us to determine the role of the AR and other key factors in regulating t-NEPC lineage plasticity.

Results: AR inhibition accentuates lineage plasticity in t-NEPC cells—an effect not observed in parental, enzalutamide-sensitive adenocarcinoma cells. Induction of an AR-repressed, lineage plasticity program is dependent on activation of the transcription factor E2F1 in concert with the BET bromodomain chromatin reader BRD4. BET inhibition (BETi) blocks this E2F1/BRD4-regulated program and decreases growth of t-NEPC tumor models and a subset of t-NEPC patient tumors with high activity of this program in a BETi clinical trial.

Conclusions: E2F1 and BRD4 are critical for activating an AR-repressed, t-NEPC lineage plasticity program. BETi is a promising approach to block this program.

Introduction

The androgen receptor (AR) is a nuclear hormone receptor that promotes luminal differentiation and growth of normal and transformed prostatic epithelial cells alike. Because of this, suppression of androgen synthesis to prevent AR activation has been the principal treatment for patients with advanced prostate cancer for nearly 80 years. A common mechanism of castration-resistant prostate cancer (CRPC) progression is intracrine androgen production (1).

Drugs such as abiraterone that reduce androgen synthesis or enzalutamide, apalutamide, or darolutamide that are AR antagonists are now approved for the treatment of men with CRPC as well as men with castration-naïve, metastatic tumors (2–10). However, resistance to AR pathway inhibition is nearly universal.

A variety of mechanisms have been identified that contribute to resistance to novel AR signaling inhibitors, including: AR gain-of-function point mutations, constitutively active AR transcript variants, AR gene amplification, and most recently, amplifications

¹Knight Cancer Institute, Oregon Health & Science University (OHSU), Portland, Oregon. ²Department of Internal Medicine, University of Michigan, Ann Arbor, Michigan. ³Rogel Cancer Center, University of Michigan, Ann Arbor, Michigan. ⁴Dana-Farber Cancer Institute, Harvard Medical School, Boston, Massachusetts. ⁵Department of Urology, University of Washington, Seattle, Washington. ⁶Divisions of Human Biology and Clinical Research, Fred Hutchinson Cancer Research Center, Seattle, Washington. ⁷Center for Drug Repurposing, Department of Internal Medicine, Department of Medicinal Chemistry, University of Michigan, Ann Arbor, Michigan. ⁸Helen Diller Family Comprehensive Cancer Center, University of California San Francisco, San Francisco, California. ⁹Genitourinary Oncology Service, Department of Medicine, Memorial Sloan Kettering Cancer Center, New York, New York. ¹⁰Department of Radiation Oncology, University Hospitals, Case Western Reserve University, Cleveland, Ohio. ¹¹Department of Computational Medicine & Bioinformatics, University of Michigan, Ann Arbor, Michigan. ¹²Department of Biostatistics, University of Michigan, Ann Arbor, Michigan. ¹³Department of Biomedical Engineering, University of Michigan, Ann Arbor, Michigan. ¹⁴Zenith Epigenetics Ltd, Calgary, Alberta, Canada.

Note: Supplementary data for this article are available at Clinical Cancer Research Online (<http://clincancerres.aacrjournals.org/>).

D.-H. Kim and D. Sun are the co-first authors of this article.

W.K. Storck, K. Welker Leng, and C. Jenkins are the co-second authors of this article.

Current address for D.-H. Kim: Department of Internal Medicine, Chonnam National University Medical School and Hwasun Hospital, Hwasun, South Korea; and current address for J.J. Alumkal, Department of Internal Medicine, Rogel Cancer Center, University of Michigan, Ann Arbor, Michigan.

Corresponding Authors: Joshi J. Alumkal, Phone: 734-936-9868; Fax: 734-647-9480; E-mail: jalumkal@med.umich.edu and Zheng Xia, Phone: 503-494-9726; E-mail: xiaz@ohsu.edu

Clin Cancer Res 2021;27:4923–36

doi: 10.1158/1078-0432.CCR-20-4968

This open access article is distributed under Creative Commons Attribution-NonCommercial-NoDerivatives License 4.0 International (CC BY-NC-ND).

©2021 The Authors; Published by the American Association for Cancer Research

Translational Relevance

The incidence of treatment-emergent neuroendocrine prostate cancer (t-NEPC) is increasing in the era of new, potent androgen receptor (AR) inhibitors. AR expression or function is commonly suppressed in t-NEPC. However, the influence of the AR on preventing this phenotype and the identity of other factors that are critical for t-NEPC's emergence are unclear. We determined that the master regulator E2F1 and the BET bromodomain protein BRD4 cooperate to activate a t-NEPC lineage plasticity program that is normally repressed by the AR. BET bromodomain inhibition (BETi) abrogates E2F1 activation of this program and suppresses growth of t-NEPC tumor models and tumors in patients with activation of this program, suggesting that E2F1- and BRD4-dependent t-NEPC tumors may be particularly susceptible to BETi.

of an enhancer upstream of the *AR* gene that regulates *AR* mRNA expression (11–14). Furthermore, posttranslational modifications of the AR or changes in AR coactivators also contribute to persistent AR function (15).

Another recent discovery is that some prostate cancer tumors have intrinsic resistance to AR-targeting agents, and these tumors appear to have lower activity of canonical AR signaling (16–18). In addition, a subset of these AR signaling inhibitor-resistant tumors exhibit lineage plasticity (19). A National Cancer Institute Panel recently defined lineage plasticity as “a biologic process that occurs during normal development and later as a mechanism that promotes cell survival when adapting to their environment, evading stress, or repairing tissues” (19). In prostate cancer, lineage plasticity is most commonly exemplified by loss of AR signaling and activation of an alternate lineage program such as neuronal differentiation (20, 21). Lineage plasticity is a spectrum with some tumors undergoing epithelial-to-mesenchymal transition, while others exhibit alternate differentiation programs divergent from a luminal program (19). Indeed, our recent studies demonstrate that approximately 17% of men with CRPC—particularly men whose tumors are resistant to drugs like enzalutamide and abiraterone—undergo lineage plasticity and lineage switching to treatment-emergent neuroendocrine prostate cancer (t-NEPC) with reduced AR function (20). The frequency of these t-NEPC tumors is much higher than *de novo* NEPC (<1% of patients; ref. 22), strongly suggesting that AR interference induces tumor adaptation by promoting lineage plasticity or leading to clonal selection.

Certain alterations, including *RB1* loss of function, are commonly found in both *de novo* and t-NEPC (20, 21). Moreover, both *de novo* and t-NEPC tumors are transcriptionally enriched for gene sets linked to neurogenesis, cell-cycle control, and activation of specific master regulator transcription factors, including E2F1, suggesting an important role for transcriptional regulation in lineage plasticity (20, 21, 23). However, there are also distinctions between *de novo* NEPC and t-NEPC. *De novo* NEPC tumors uniformly exhibit loss of AR expression (21). However, the influence of AR loss on the development of *de novo* NEPC is unclear because this loss occurs concomitantly with the diagnosis of *de novo* NEPC. Conversely, many t-NEPC tumors progressing on enzalutamide and abiraterone retain AR expression; however, transcriptional measurements indicate that the AR's function is suppressed (20). This suggests that loss of AR function may contribute to the emergence of t-NEPC. Finally, targetable proteins that promote lineage plasticity and survival of t-NEPC or other AR activity-low prostate cancer subsets are largely unknown, demonstrating an unmet clinical need.

To identify mechanisms that contribute to t-NEPC lineage plasticity, we used an integrative systems biology approach and focused on AR activity-low, enzalutamide-resistant cell lines with persistent AR expression that exhibit features of t-NEPC lineage plasticity (24). Importantly, while these AR activity-low, enzalutamide-resistant cells have transcriptional and chromatin features of t-NEPC at baseline, enzalutamide treatment of these cells—but not parental, enzalutamide-sensitive adenocarcinoma cells—further promotes t-NEPC lineage plasticity. This effect is related to activation of AR-repressed genes that we find to be upregulated in t-NEPC patient tumors. We propose that activation of this AR-repressed program is critical for accentuating t-NEPC lineage plasticity. Critically, we determined that the BET bromodomain protein BRD4 cooperates with the master regulator transcription factor E2F1 to activate this t-NEPC lineage plasticity program and that BET bromodomain inhibition (BETi) blocks this program and decreases t-NEPC cell survival. Corroborating our preclinical results, we determined that t-NEPC tumors from patients treated on a BETi clinical trial that express high levels of E2F1 and BRD4 or that have activation of the AR-repressed, t-NEPC lineage plasticity program appear to derive the greatest benefit from BETi. These findings support the therapeutic potential of BETi in a subset of patients whose tumors have undergone a t-NEPC lineage switch.

Materials and Methods

Metastatic tissue collection

We collected human metastatic tissues after Institutional Review Board-approval at the participating sites. We obtained informed, written patient consent from all subjects. Study enrollment and procedures were consistent with the Declaration of Helsinki.

Cell culture

LNCAp cells were purchased from ATCC (CRL-1740). V16D, MR42D, MR42F, ResA, DKO, and TKO were described previously (24–26). LNCAp and V16D cells were grown in RPMI1640 (Gibco) supplemented with 10% FBS (Premium Select grade, Atlanta Biologicals). MR42D, MR42F, and ResA cells were grown in RPMI + 10% FBS and 10 μ mol/L enzalutamide (MedChemExpress #HY-70002). DKO and TKO were grown in DMEM/high glucose with l-glutamine, sodium pyruvate (Cytiva) + 10% FBS. For MR42D and MR42F washout conditions, the cells were grown for 72 hours in the absence of enzalutamide prior to subsequent treatments.

Data availability

The RNA sequencing (RNA-seq), ChIP sequencing (ChIP-seq), and ATAC sequencing (ATAC-seq) datasets reported in this article are available in the NCBI Gene Expression Omnibus (GEO) using accession number GSE147877.

Details of experimental procedures for other methods, including: cell viability assays, transfections, RT-qPCR, immunoblotting, chromatin immunoprecipitation, genomic and epigenomic profiling, data analysis, and statistical analysis are included in the Supplementary Materials and Methods.

Results

Enzalutamide treatment of AR-expressing t-NEPC cells accentuates lineage plasticity

Prior work suggested that canonical AR transcriptional function is suppressed in t-NEPC tumors, including subsets of t-NEPC tumors with persistent expression of the AR (20). Notably, many of these

AR-expressing t-NEPC tumors were obtained from patients who were still taking AR signaling inhibitors such as enzalutamide or abiraterone at the time of biopsy (20), suggesting that continued drug treatment may have contributed to suppression of AR function and emergence of this phenotype. However, it is not clear what direct functional role the AR plays in restraining the t-NEPC phenotype due to insufficient models to study this question.

Previously, Bishop and colleagues determined that a subset of enzalutamide-resistant, AR activity–low, LNCaP-derived CRPC cell lines (e.g., MR42D and MR42F) exhibit persistent AR expression but also expression of NEPC genes versus enzalutamide-sensitive, adenocarcinoma LNCaP or related LNCaP-derived CRPC, enzalutamide-sensitive V16D cells (24). Using RNA-seq, we confirmed that a signature (21) used previously to distinguish t-NEPC patient tumors from adenocarcinoma patient tumors was highly activated in MR42D and MR42F but not in V16D or LNCaP cells (Fig. 1A).

The AR protein is still highly expressed in V16D, MR42D, and MR42F; however, PSA expression is low while the neuronal marker neural cell adhesion molecule 1 (NCAM1) is highly expressed in MR42D and MR42F but not in V16D cells, further demonstrating the t-NEPC phenotype of MR42D and MR42F (Fig. 1B; ref. 24). To determine whether enzalutamide affected important cancer hallmarks in these cells, including proliferation and differentiation, we treated MR42D or MR42F that had been washed out of enzalutamide for 72 hours (enzalutamide-washout) or V16D cells with enzalutamide and measured changes in cell viability. Enzalutamide blocked proliferation most significantly in V16D cells compared with the MR42D and MR42F enzalutamide-washout cells (Fig. 1C). AR siRNA experiments corroborated these results and demonstrated that MR42D and MR42F are not dependent on the AR for proliferation (Supplementary Fig. S1A). Importantly, enzalutamide treatment reduced PSA expression in all cell lines (Fig. 1D). Significantly, enzalutamide further increased expression of the neuronal marker NCAM1 exclusively in MR42D and MR42F cells, but not V16D cells (Fig. 1D)—an effect recapitulated with apalutamide (Supplementary Fig. S1B)—suggesting that AR interference may accentuate t-NEPC lineage plasticity in these cells.

We next sought to identify gene expression changes induced by AR interference in t-NEPC versus adenocarcinoma cells. Therefore, we treated MR42D and MR42F enzalutamide-washout cells as well as LNCaP and V16D cells with enzalutamide for 24 hours and performed RNA-seq. Gene set enrichment analysis (GSEA) using the Hallmark pathways demonstrated that the top deactivated pathway with enzalutamide in MR42D, MR42F, V16D, and LNCaP was AR signaling (Fig. 1E; Supplementary Fig. S1C; Supplementary Table S1), confirming on-target effects of enzalutamide on blocking canonical AR signaling and demonstrating target engagement across the models.

Because AR interference activated expression of the neuronal marker NCAM1 in MR42D and MR42F—but not V16D—we next focused on pathways activated by enzalutamide in MR42D or MR42F but not in LNCaP or V16D and determined whether these unique pathways were linked to t-NEPC lineage plasticity. Several gene sets met these criteria, including those shown previously to be enriched in AR activity–low or t-NEPC tumors such as: epithelial-to-mesenchymal transition (EMT), IFN response, apoptosis, mitotic spindle, or E2F targets (Supplementary Table S1; refs. 16, 20, 21). Furthermore, gene ontology (GO) pathway analysis demonstrated that enzalutamide treatment activated multiple gene sets linked to neuronal development or differentiation exclusively in MR42D or MR42F, but not LNCaP or V16D (Supplementary Table S1).

Specific AR-repressed target genes are enriched in t-NEPC patient tumors and promote t-NEPC cell survival

We next focused on identifying direct, AR-repressed target genes uniquely activated by enzalutamide in t-NEPC cells but not in LNCaP or V16D. We focused on MR42D and identified 1,542 genes that were uniquely activated by enzalutamide in our RNA-seq data (Supplementary Table S2). To determine whether AR directly regulates the expression of these unique enzalutamide-induced genes, we treated MR42D enzalutamide-washout cells with vehicle or enzalutamide for 24 hours and performed AR ChIP-seq. Analysis of nuclear and cytoplasmic protein extractions confirmed that enzalutamide depleted the AR from the nucleus (Supplementary Fig. S2A), and AR ChIP-seq demonstrated that enzalutamide reduced AR DNA occupancy (Supplementary Fig. S2B). By integrating the 2,462 genes from which AR was evicted from our ChIP-seq analysis with the genes uniquely induced with enzalutamide treatment in MR42D versus LNCaP and V16D, we identified 76 direct, AR-repressed target genes (Fig. 2A; Supplementary Table S2). Functional enrichment analysis determined that the top 10 pathways associated with these 76 genes were linked to neuronal development or differentiation, further suggesting that the AR represses genes linked to neurogenesis in MR42D t-NEPC cells (Fig. 2B). This lineage plasticity gene program was also significantly activated by enzalutamide in MR42F cells (Supplementary Fig. S2C), demonstrating its relevance in another t-NEPC lineage plasticity model. Furthermore, this lineage plasticity gene program was activated in several other models of AR activity loss or NEPC lineage plasticity—all of which are E2F1 activity–high—including: enzalutamide-resistant ResA, TRAMP NEPC mouse tumors, and *PTEN/RB1* double knock out (DKO) and *PTEN/RB1/TP53* triple knockout (TKO) NEPC mouse tumors (Supplementary Fig. S2D–S2F; refs. 25–27).

To determine the clinical significance of the 76 AR-repressed genes identified in our integrative analysis, we examined their expression in two publicly available CRPC datasets that include both t-NEPC and adenocarcinoma tumors (20, 21). The 76-gene, AR-repressed program was enriched in t-NEPC versus adenocarcinoma in both datasets (Fig. 2C). Furthermore, we examined matched biopsies from 3 patients treated with enzalutamide whose baseline tumors were adenocarcinoma but whose progression tumors following enzalutamide treatment had undergone t-NEPC lineage plasticity (28). Genes from the AR-repressed gene program were significantly higher in the enzalutamide-resistant t-NEPC tumors versus the baseline adenocarcinoma tumors (Fig. 2D; Supplementary Fig. S2G). These data strongly suggest that the emergence of t-NEPC after enzalutamide treatment coincides with activation of the AR-repressed, t-NEPC lineage plasticity gene program we identified.

Our integrative analysis identified a clinically relevant program of AR-repressed genes—many of which were associated with neurogenesis—that were higher in expression in tumor models and patient tumors that had undergone t-NEPC lineage plasticity. To further confirm our RNA-seq results implicating the t-NEPC lineage plasticity program, we performed RT-qPCR analysis using RNA from MR42D washout cells versus V16D cells treated with vehicle or enzalutamide. We focused on several genes that were linked previously to neuronal differentiation or survival of AR activity–low cells: *BCL2*, *MET*, *KIAA0319*, and *CHAC1* (17, 29–32). Enzalutamide decreased expression of the AR-activated gene *KLK3* in both V16D and MR42D; however, enzalutamide increased the expression of *BCL2*, *MET*, *KIAA0319*, and *CHAC1* only in MR42D (Fig. 2E; Supplementary Fig. S2H). We additionally confirmed that increased *BCL2* and *MET* mRNA expression with enzalutamide treatment corresponded to increased protein expression (Supplementary Fig. S2I). *BCL2* and

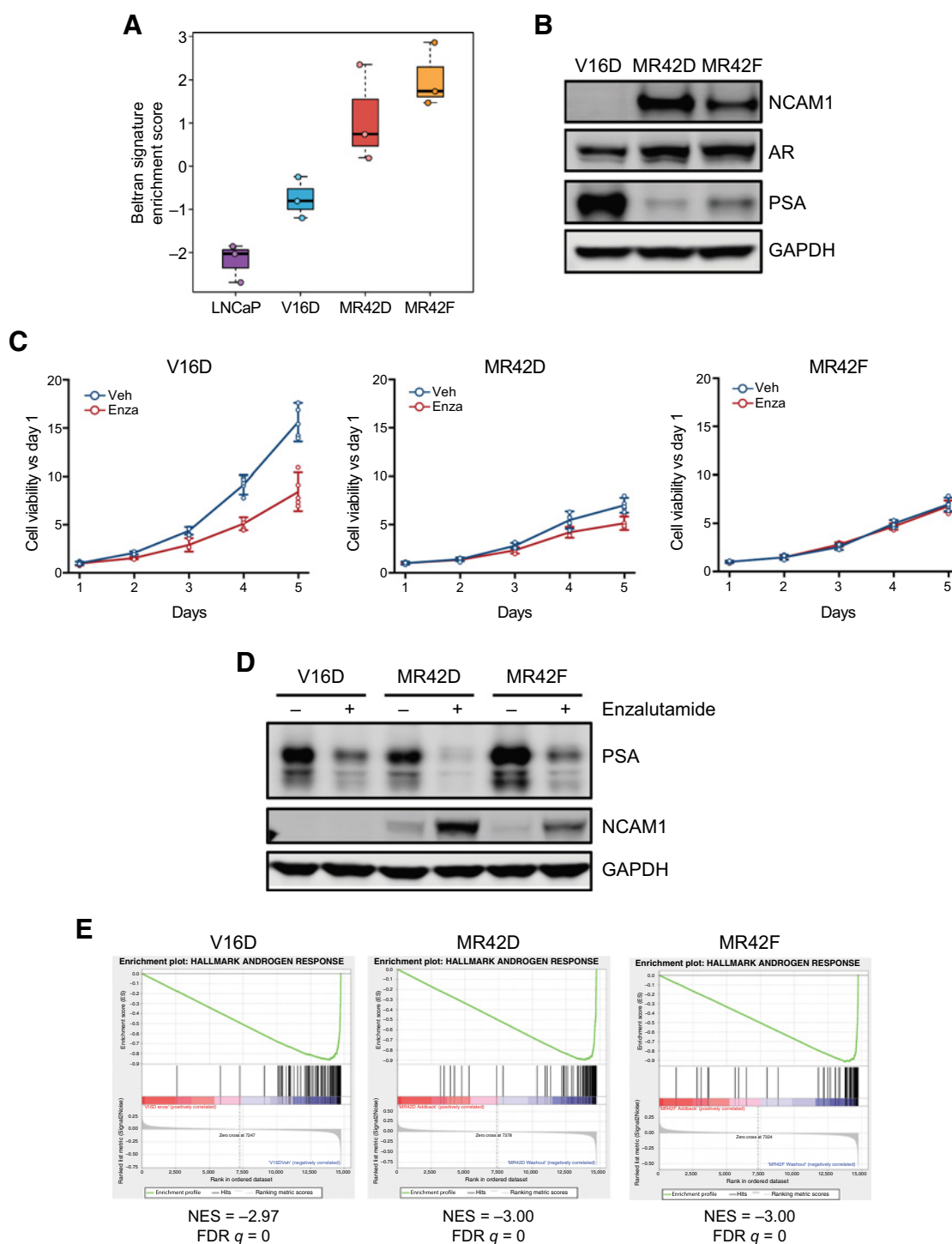


Figure 1.

Enzalutamide treatment of AR-expressing t-NEPC cells accentuates lineage plasticity. **A**, Beltran NEPC signature enrichment scores in LNCaP, V16D, MR42D, and MR42F cells. The difference in scores between cell lines is significant ($P = 0.02$ by the Kruskal-Wallis test). **B**, Western blot depicting NCAM1, AR, PSA, and GAPDH levels in V16D cells and MR42D and MR42F enzalutamide-maintenance cells. **C**, Cell viability of V16D cells or MR42D and MR42F enzalutamide-washout cells was measured at the indicated time points posttreatment with vehicle (veh) or 10 $\mu\text{mol/L}$ enzalutamide using live/dead cell counting. Data are reported as individual replicates ($n = 5$) \pm 95% confidence interval, and two-tailed Student t tests were performed; V16D $P = 0.0001$, MR42D $P = 0.001$, MR42F $P = 0.5$. **D**, Western blots depicting PSA, NCAM1, and GAPDH levels in V16D, MR42D, and MR42F whole-cell lysates from **C**. **E**, GSEA enrichment plots of the Hallmark pathway androgen response using RNA-seq from V16D, MR42D, and MR42F cells treated with 10 $\mu\text{mol/L}$ enzalutamide or vehicle for 24 hours.

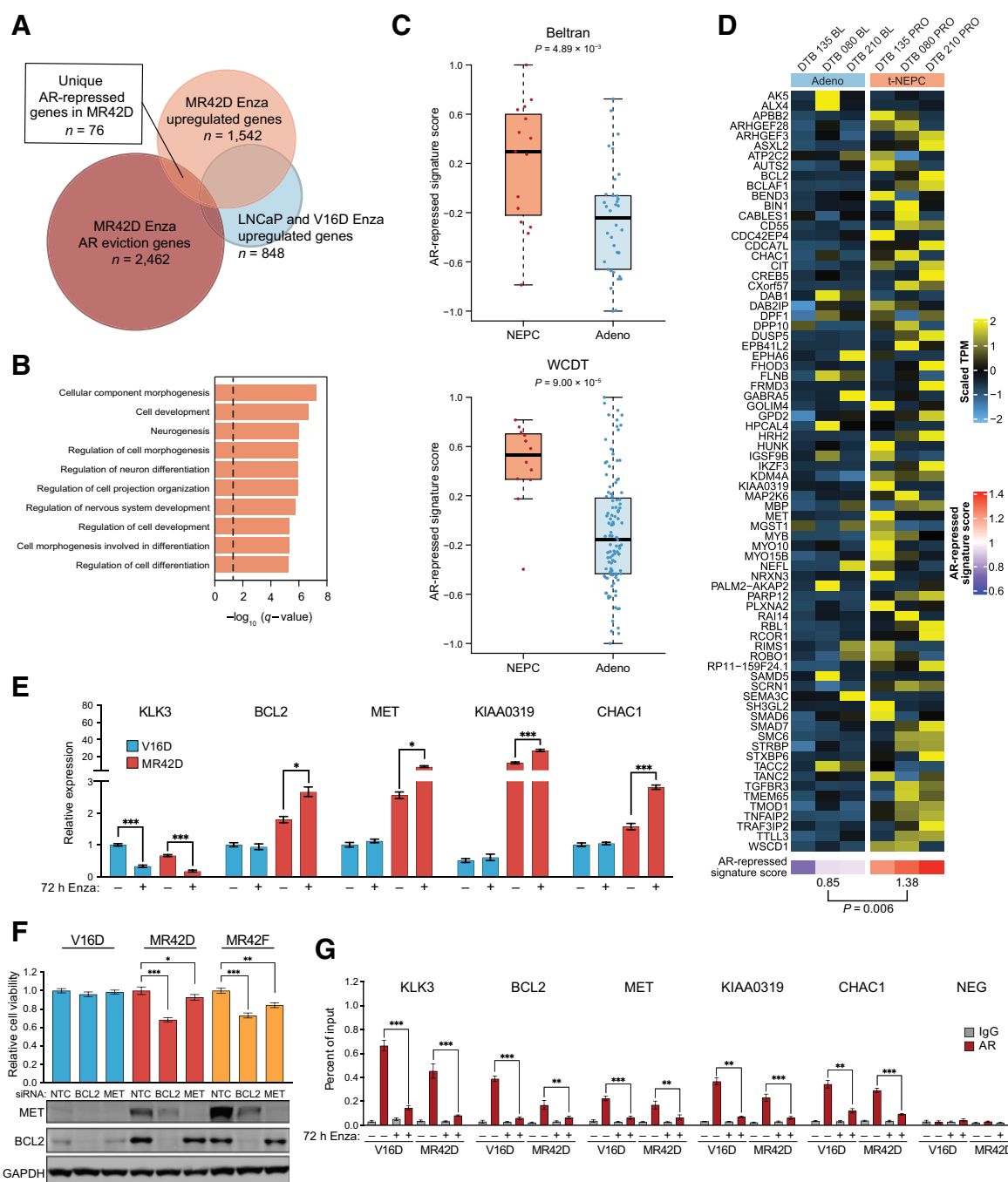


Figure 2.

Specific AR-repressed target genes are enriched in t-NEPC patient tumors and promote t-NEPC cell survival. **A**, Venn diagram of the upregulated, differentially expressed genes (DEGs) by RNA-seq in MR42D enzalutamide-washout cells and V16D or LNCaP cells treated with enzalutamide (FDR<0.05), and genes identified by ChIP-seq where AR binding was reduced in MR42D washout cells treated with enzalutamide ($P < 0.001$; fold enrichment > 4). Seventy-six unique, AR-repressed genes were identified by comparing the exclusively upregulated DEGs in MR42D (but not LNCaP and V16D) and AR-evicted genes. **B**, Top 10 enriched pathways for the 76 unique, AR-repressed genes in MR42D as determined by the MSigDB enrichment tool (see Methods). The dashed line corresponds to $q = 0.05$. **C**, The single-sample gene-set variation analysis (GSVA) score of 76 unique, AR-repressed genes in Beltran and WCDT datasets. **D**, Heatmap depicting scaled TPM gene expression of AR-repressed genes from **A** in matched biopsies from three patients with baseline adenocarcinoma tumors treated with enzalutamide whose progression biopsies showed t-NEPC. **E**, Validation of gene expression changes with enzalutamide treatment by RT-qPCR at *KLK3* and selected t-NEPC genes. Gene expression was normalized to a *GAPDH* internal control ($n = 3$). **F**, Relative viability of V16D cells or MR42D and MR42F enzalutamide-maintenance cells 72 hours after introducing *MET*, *BCL2*, or NTC siRNA oligonucleotides (top; $n = 6$). Western blots indicate protein levels (bottom). **G**, Validation of AR occupancy data by ChIP-qPCR at *KLK3* and selected t-NEPC genes. UNTR4 region was used as a negative control (NEG; $n = 3$). In **E** and **G**, V16D cells or MR42D enzalutamide-washout cells were treated with vehicle or 10 $\mu\text{mol/L}$ enzalutamide for 72 hours. Data are reported as the average \pm SD, and two-tailed Student *t* tests were performed (*, $P < 0.05$; **, $P < 0.01$; ***, $P < 0.001$).

MET have been previously linked to promoting survival of AR-independent CRPC (29, 30). To determine the functional significance of these genes, we used siRNA to suppress their expression. siRNA-mediated suppression of each gene reduced survival of MR42D and MR42F but not V16D cells (Fig. 2F), demonstrating the importance of these AR-repressed, enzalutamide-activated genes in t-NEPC lineage plasticity.

To determine whether the AR uniquely binds regulatory elements of these AR-repressed genes in MR42D, we treated MR42D enzalutamide-washout cells or V16D cells with vehicle or enzalutamide and performed ChIP-qPCR using primers for *KLK3*, *BCL2*, *MET*, *KIAA0319*, and *CHAC1* gene regions from our ChIP-seq where AR was depleted by enzalutamide in MR42D cells (Supplementary Fig. S2J). Our results show that AR was bound to the regulatory element of the AR-activated gene *KLK3* in both MR42D and V16D, and enzalutamide reduced AR binding to *KLK3* at 24 and 72 hours (Fig. 2G; Supplementary Fig. S2K). Significantly, enzalutamide also reduced AR binding at *BCL2*, *MET*, *KIAA0319*, and *CHAC1* in both V16D and MR42D at both time points (Fig. 2G; Supplementary Fig. S2K).

The chromatin state of enzalutamide-resistant t-NEPC cells is conducive to lineage plasticity gene expression

AR eviction from chromatin was not sufficient to explain activation of the t-NEPC lineage plasticity program in MR42D cells (Fig. 2G; Supplementary Fig. S2K). We hypothesized that differences in chromatin accessibility in the ground state may contribute to neuronal gene activation following AR suppression. Therefore, we performed assay for transposase-accessible chromatin sequencing (ATAC-seq) in MR42D enzalutamide-washout cells and V16D cells. We used GSEA to define the top gene sets associated with hyper-accessible regions in each cell line. Nearly all of the top gene sets enriched in hyper-accessible regions in MR42D were associated with neuronal pathways (Fig. 3A). Conversely, the top gene sets enriched in hyper-accessible regions in V16D cells were associated with metabolic pathways (Fig. 3A). These results demonstrate that MR42D cells have a chromatin hyper-accessibility profile that favors t-NEPC lineage plasticity, a process accentuated by AR interference.

We hypothesized that activation of specific factors may explain how t-NEPC lineage plasticity is accentuated with enzalutamide treatment of MR42D, but not V16D. Histone acetylation is linked to gene activation and lineage commitment (33). Therefore, we set out to determine whether changes in histone acetylation contributed to gene expression changes induced by AR suppression in MR42D. We treated MR42D enzalutamide-washout cells with either enzalutamide or vehicle and then performed H3K27 acetylation (H3K27ac) ChIP-seq. Enzalutamide treatment dynamically increased H3K27ac levels at regulatory regions corresponding to t-NEPC lineage plasticity genes (Fig. 3B). These results suggest that the chromatin profile of MR42D cells may contribute to enzalutamide-induced activation of genes highly expressed in t-NEPC.

The H3K27ac chromatin mark is recognized by BET bromodomain proteins, including BRD4, an important chromatin reader and regulator of lineage commitment (33). To determine whether enzalutamide treatment impacted BRD4 binding, we performed BRD4 ChIP-seq. There was a strong colocalization of increased H3K27ac and BRD4 signals (Fig. 3B; Supplementary Fig. S3A), and these two signals were highly correlated (Pearson correlation $r = 0.76$, $P < 1 \times 10^{-15}$). To confirm our ChIP-seq findings, we treated V16D cells or MR42D enzalutamide-washout cells with vehicle or enzalutamide and performed ChIP-qPCR. Enzalutamide increased H3K27ac and BRD4

binding at *BCL2*, *MET*, *KIAA0319*, and *CHAC1* genes in MR42D cells, but not in V16D cells (Fig. 3C and D; Supplementary Fig. S3B and S3C). These results suggest that H3K27ac and BRD4 occupancy enhances t-NEPC lineage plasticity and that other cooperating factors may also be important.

BET bromodomain proteins cooperate with specific master regulator transcription factors to promote gene expression and lineage commitment (33, 34). To identify factors that may cooperate with BRD4, we first performed functional enrichment analysis of the shared H3K27ac and BRD4 peaks in the enzalutamide condition. This analysis showed a strong enrichment for pathways previously linked to t-NEPC lineage plasticity, including Myc targets, E2F targets, and G2-M checkpoint genes (Supplementary Fig. S3D; refs. 20, 21). To further define transcription factors whose activation state was uniquely modulated in MR42D and MR42F, we used RNA-seq data from MR42D, MR42F, V16D, and LNCaP cells treated with enzalutamide or vehicle and performed master regulator transcription factor analysis using the Virtual Inference of Protein-activity (VIPER) algorithm (16, 35). Importantly, VIPER predicted that enzalutamide deactivated AR function in all cell lines, corroborating our GSEA results (Supplementary Table S3; Fig. 1E; Supplementary Fig. S1C). In examining the top 10 transcription factors predicted to be activated by enzalutamide in each line, only E2F1 was uniquely activated in MR42D and MR42F but not V16D and LNCaP (Supplementary Table S3). Indeed, enzalutamide treatment of V16D and LNCaP was predicted to deactivate E2F1 (Supplementary Table S3). This is consistent with our results showing activation of the AR-repressed, lineage plasticity program in other AR activity-low, E2F1 activity-high models (Supplementary Fig. S2D–S2F) and strongly suggests that E2F1 may be important for activation of this program.

E2F1 activates a t-NEPC lineage plasticity gene expression program and confers enzalutamide resistance

We and others previously showed that E2F1's gene sets are highly enriched in human t-NEPC versus adenocarcinoma patient tumors (20, 23). In addition, our prior work using master regulator analysis also implicated E2F1 activation in t-NEPC versus adenocarcinoma CRPC patient tumors (20, 28). Furthermore, E2F1 activation has been strongly linked to stemness and associated with NEPC lineage plasticity (20, 23, 25, 26, 36). Therefore, we sought to determine E2F1's importance for the AR-repressed, t-NEPC lineage program we identified. *E2F1* was more highly expressed in human t-NEPC patient tumors versus adenocarcinoma in two datasets (Fig. 4A; refs. 20, 21). We also examined *E2F1* expression in matched biopsies from patients whose baseline tumors were adenocarcinoma but whose progression tumors following enzalutamide treatment were t-NEPC (Fig. 2D). *E2F1* expression was increased in two of the three t-NEPC progression samples after enzalutamide treatment (Supplementary Fig. S4A). Moreover, E2F1 protein and mRNA expression were higher in t-NEPC MR42D and MR42F cells versus V16D adenocarcinoma cells (Fig. 4B), as was nuclear localization of E2F1 protein (Supplementary Fig. S4B). To determine mechanisms that contribute to *E2F1* upregulation in t-NEPC cells, we performed ChIP-qPCR for H3K27ac and BRD4. Importantly, H3K27ac levels and BRD4 binding were higher at the *E2F1* promoter in MR42D versus V16D (Fig. 4C), suggesting that BRD4 may contribute to *E2F1* upregulation. In keeping with that notion, there was a strong correlation with *BRD4* and *E2F1* expression in published human CRPC datasets, especially in t-NEPC tumors (Fig. 4D; refs. 20, 21). Finally, like *E2F1* expression (Fig. 4A), *BRD4* expression was increased in t-NEPC samples (Supplementary Fig. S4C), including patient tumor samples that had undergone

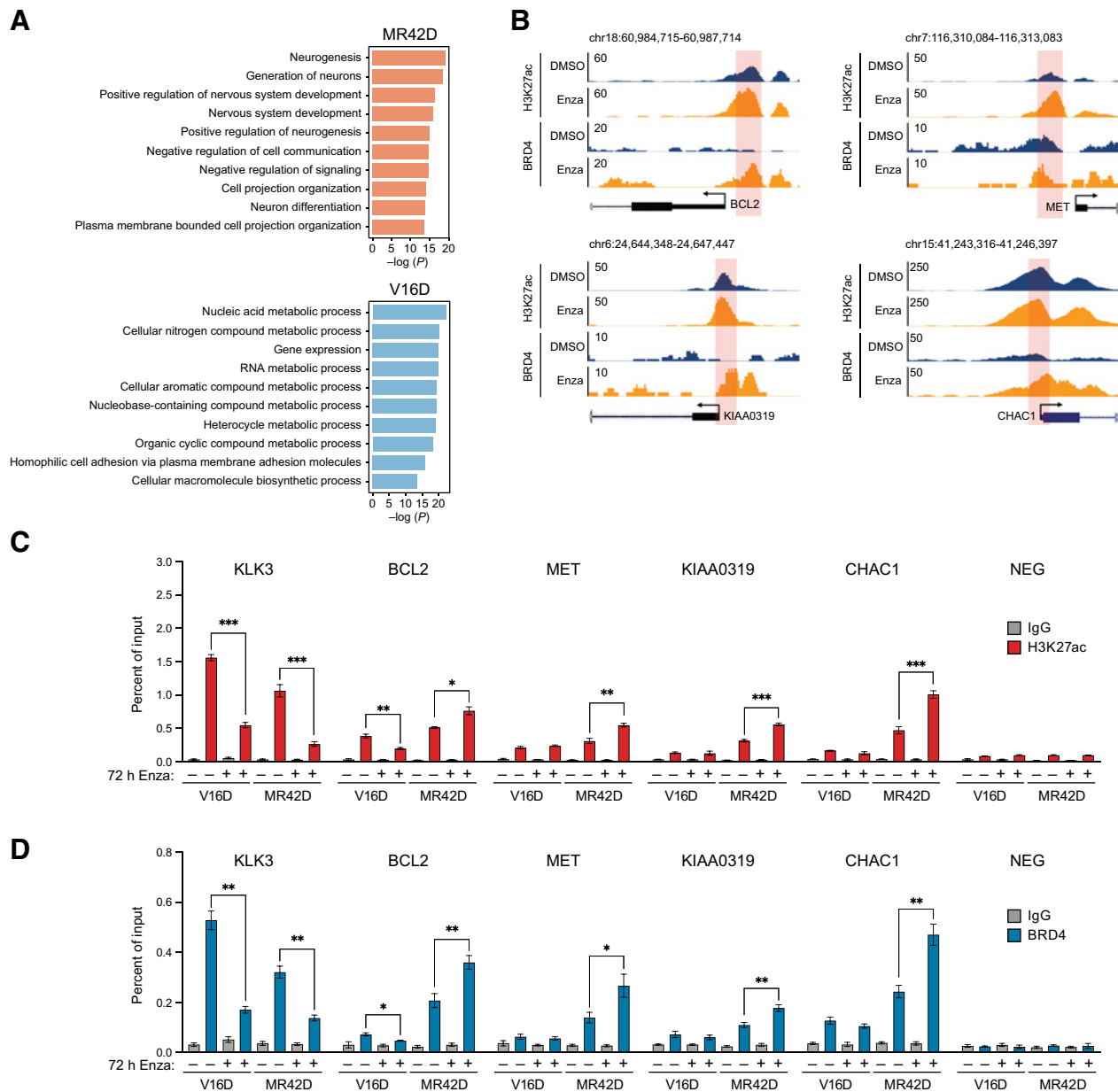


Figure 3.

The chromatin state of enzalutamide-resistant t-NEPC cells is conducive to lineage plasticity gene expression. **A**, The top 10 pathways enriched in ATAC-seq hyper-accessible peaks in MR42D enzalutamide-washout cells or V16D cells. **B**, Alignment of representative genome browser views from H3K27ac and BRD4 ChIP-seq for the indicated genes. Depicted datasets include H3K27ac and BRD4 ChIP-seq of MR42D enzalutamide-washout cells treated with vehicle or 10 μ mol/L enzalutamide for 24 hours. **C**, H3K27ac ChIP-qPCR showing levels of H3K27ac at the indicated genes in V16D or MR42D cells. **D**, BRD4 ChIP-qPCR showing BRD4 occupancy levels at the indicated genes in V16D or MR42D cells. In **C** and **D**, V16D cells or MR42D enzalutamide-washout cells were treated with vehicle or 10 μ mol/L enzalutamide for 72 hours. UNTR4 region was used as a negative (NEG) control region ($n = 3$). Data are reported as the average \pm SD, and two-tailed Student *t* tests were performed (*, $P < 0.05$; **, $P < 0.01$; ***, $P < 0.001$).

t-NEPC lineage plasticity after enzalutamide treatment (Supplementary Fig. S4A). These results suggest E2F1 and BRD4 may cooperate to promote t-NEPC lineage plasticity.

To determine whether E2F1 was necessary and sufficient for activating genes highly expressed in t-NEPC, we performed gain-of-function experiments in V16D and LNCaP and loss-of-function experiments in MR42D and MR42F. While enzalutamide treatment

and AR eviction were insufficient to increase expression of t-NEPC genes in V16D cells at 24 or 72 hours (Fig. 2E and G; Supplementary Fig. S2H, S2I, and S2K), E2F1 overexpression was sufficient to increase expression of genes highly expressed in t-NEPC in both V16D and LNCaP cells (Fig. 4E; Supplementary Fig. S4D). Using ChIP-qPCR assays, we confirmed that E2F1 overexpression led to increased E2F1 occupancy at promoter elements for these genes and that E2F1 binding

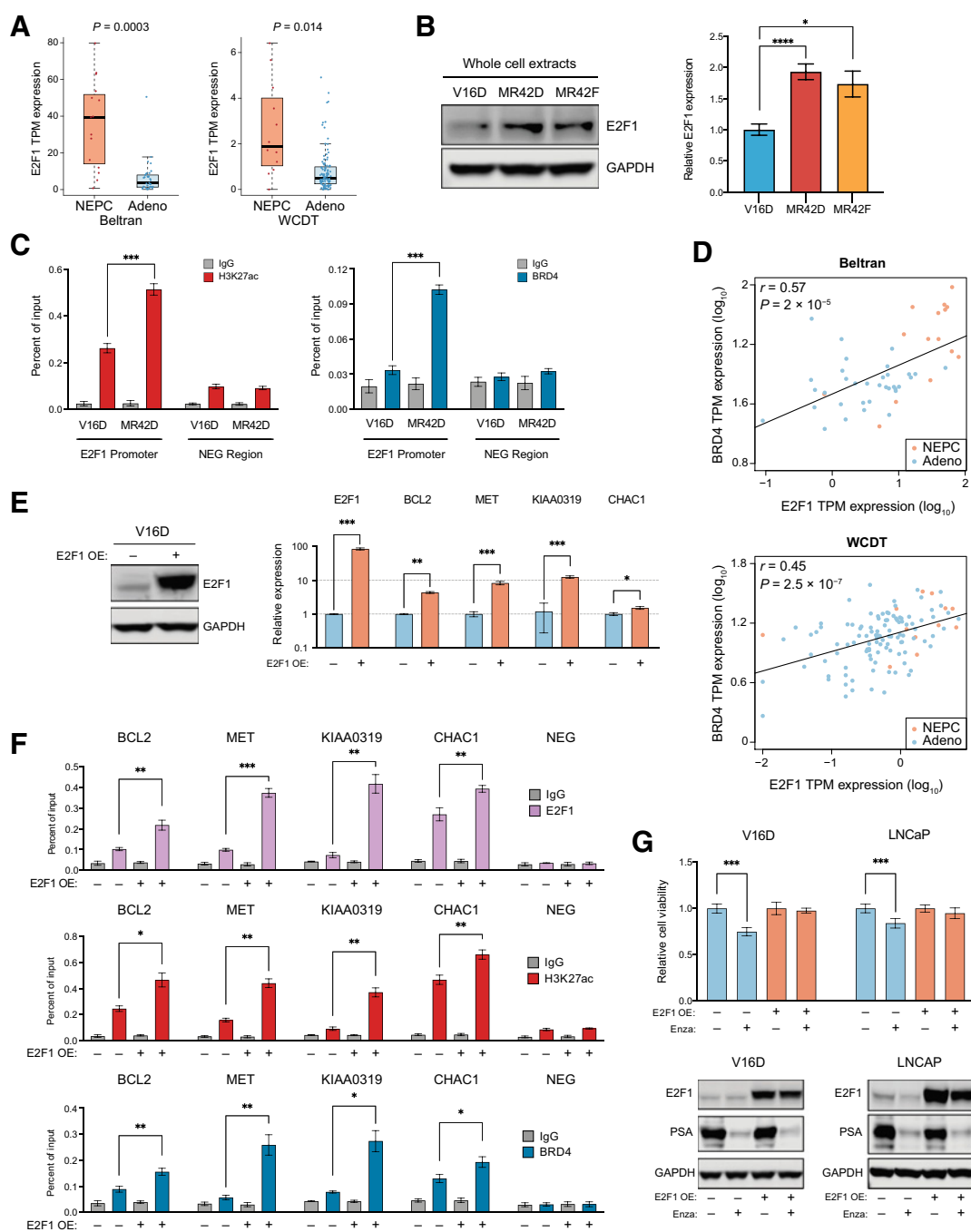


Figure 4.

E2F1 activates a t-NEPC lineage plasticity gene expression program and confers enzalutamide resistance. **A**, Box plots of *E2F1* expression in t-NEPC compared with adenocarcinoma tumors from Beltran (ref. 21; left) and WCDT (ref. 20; right) patient datasets. The *P* values were determined by Student *t* test using the \log_2 -transformed TPM values. **B**, Western blot of E2F1 and GAPDH in V16D or MR42D and MR42F enzalutamide-maintenance whole-cell extracts (left). Relative *E2F1* mRNA expression in V16D cells and MR42D and MR42F enzalutamide-maintenance cells (right). *E2F1* was normalized to *GAPDH* ($n = 3$). The protein lysates used are from the same experiment shown in **Fig. 1B**. The same GAPDH blot serves as a loading control for both **Figs. 1B** and **4B**. **C**, ChIP-qPCR showing relative enrichment of H3K27ac (left) and BRD4 (right) at the *E2F1* promoter in V16D and MR42D cells. **D**, Scatter plots and linear fitted lines of log-transformed TPM expression of *BRD4* and *E2F1* in samples from the Beltran (top) or WCDT (bottom) datasets. Pearson correlation coefficients (*r*) and *P* values are shown. **E**, V16D cells were harvested 48 hours after transient transfection with empty vector (EV; E2F1 OE -) or E2F1 OE plasmids (E2F1 OE +). Western blot of E2F1 OE (left). RT-qPCR of the indicated genes in EV or E2F1 OE V16D cells ($n = 3$; right). **F**, ChIP-qPCR showing relative enrichment of E2F1, H3K27ac, and BRD4 at t-NEPC gene promoters 48 hours after transient E2F1 overexpression in V16D cells. **G**, Relative viability of V16D or LNCaP cells 72 hours after transfection with EV or E2F1 OE plasmids treated with DMSO (-) or 10 $\mu\text{mol/L}$ enzalutamide (+) for the final 66 hours ($n = 6$; top). Western blots of indicated protein expression (bottom). In **B** and **C**, and **E-G**, data are reported as average \pm SD. Two-tailed Student *t* tests were performed (*, $P < 0.05$; **, $P < 0.01$; ***, $P < 0.001$; ****, $P < 0.0001$).

coincided with increased levels of H3K27ac and BRD4, strongly suggesting cooperation between these factors at chromatin (Fig. 4F).

E2F1 overexpression in V16D and LNCaP cells also conferred resistance to enzalutamide, and this effect was not due to maintenance of AR function based on levels of PSA expression (Fig. 4G). Further supporting a role for E2F1 in t-NEPC lineage plasticity, E2F1 siRNA reduced viability of MR42D and MR42F cells but not V16D cells (Supplementary Fig. S4E), and E2F1 siRNA in t-NEPC cells reduced expression of lineage plasticity genes (Supplementary Fig. S4F).

BET bromodomain inhibition blocks E2F1 function, t-NEPC lineage plasticity gene expression, and t-NEPC cell survival

Our integrative analysis and cell-based experiments suggested that E2F1 cooperates with BRD4 to activate expression of genes that are highly expressed in t-NEPC. Although E2F1 is not currently targetable, BET bromodomain inhibitors (BETi) have been developed and are currently in clinical testing (NCT02711956). Therefore, we sought to determine the antitumor activity of BETi in t-NEPC and whether those effects were linked to suppression of E2F1 function.

First, we treated MR42D and MR42F with three chemically different drugs that block BET bromodomain function: JQ1, a pan-BETi; ARV-771, a pan-BET degrader (BETd) that causes BRD4 degradation; and ZEN-3694, a pan-BETi currently undergoing clinical investigation. Importantly, each drug reduced expression of E2F1 and AR-repressed lineage plasticity genes implicated in our analyses (Fig. 5A). We confirmed these results using AR activity–low, E2F1 activity–high ResA cells (25), in which JQ1 and ZEN-3694 similarly blocked these genes' expression (Supplementary Fig. S5A).

BETi act by binding to the bromodomains of BRD4 and interfering with its recruitment to acetylated histones on chromatin (37, 38). To confirm this effect, we treated MR42D cells with JQ1 and then performed BRD4 ChIP-qPCR. JQ1 treatment evicted BRD4 from *E2F1*, *BCL2*, *MET*, *KIAA0319*, and *CHAC1* regulatory elements, demonstrating that BRD4 inhibition is linked to reduced expression of these genes (Fig. 5B).

Next, we sought to determine whether E2F1 activation of genes highly expressed in t-NEPC was dependent on BET bromodomain proteins. JQ1 reduced expression of an E2F1-driven reporter construct, and this effect was linked to reduced E2F1 mRNA and protein expression (Supplementary Fig. S5B and S5C). Furthermore, while E2F1 overexpression increased *BCL2*, *MET*, *KIAA0319*, and *CHAC1* expression, JQ1 abrogated those effects (Fig. 5C; Supplementary Fig. S5D). Importantly, the abrogation of E2F1 function by JQ1 was not linked to changes in ectopic E2F1 expression (Fig. 5C; Supplementary Fig. S5D), suggesting that BET bromodomain proteins may regulate E2F1 function independently of E2F1 expression.

To more comprehensively identify gene expression changes linked to BET bromodomain interference, we treated MR42D cells with either the BETi JQ1 or the BETd ARV-771 and performed RNA-seq. As predicted, because ARV-771 is a BRD4 degrader, ARV-771 reduced BRD4 protein levels while JQ1 did not (Supplementary Fig. S5E). Importantly, many of the genes downregulated by ARV-771 and JQ1 were shared (Fig. 5D; Supplementary Table S4). We sought to determine the influence of these treatments on AR-repressed genes important for t-NEPC lineage plasticity. Therefore, we compared the list of genes downregulated by both ARV-771 and JQ1 versus genes induced by enzalutamide treatment of MR42D cells. The expression of 519 genes was decreased by both JQ1 and ARV-771 but increased with enzalutamide (Fig. 5D; Supplementary Table S4). The top pathway of the intersecting genes was linked to E2F1, followed by other pathways previously implicated in t-NEPC, including EMT, G₂-M, and apo-

ptosis (Fig. 5E; refs. 20, 21). Furthermore, using VIPER, we determined that E2F1 was the top transcription factor predicted to be deactivated by both JQ1 and ARV-771, further suggesting cooperativity between E2F1 and BET proteins (Supplementary Table S5). Importantly, the neural transcription factor POU3F2 has been linked previously to survival of t-NEPC cells, including MR42D and MR42F (24). However, master regulator analysis did not implicate POU3F2 as being deactivated by JQ1 or ARV-771 (Supplementary Table S5).

Prior work demonstrated that BETi is a promising approach to block growth of AR-driven tumors (37), and we recently extended these findings and confirmed the antitumor activity of BETi in AR-null adenocarcinoma CRPC (34, 38). Thus, we sought to determine the antitumor activity of BETi in t-NEPC cells or those with low AR activity but high E2F1 activity. Treatment of MR42D or MR42F with BETi suppressed growth of these cells in a dose-dependent manner (Fig. 5F; Supplementary Fig. S5F). Furthermore, BETi treatment of ResA cells, *PTEN/RB1* DKO and *PTEN/RB1/TP53* TKO knockout mouse NEPC cell lines (26), and t-NEPC patient-derived organoids WCM154 and WCM155 (39) recapitulated this effect (Fig. 5F). Finally, we treated AR-null t-NEPC LuCaP patient-derived xenograft cultures *in vitro* with JQ1 or ZEN-3694. These LuCaP cultures do not proliferate well long-term, but BETi treatment using concentrations $\leq 1 \mu\text{mol/L}$ of either agent led to cell death (Supplementary Fig. S5G). BRD4 siRNA also reduced cell survival of MR42D and MR42F and suppressed expression of E2F1-activated t-NEPC lineage plasticity genes, recapitulating the effects of BETi treatment and suggesting that interference with BRD4 contributes to the antitumor effects of BETi (Supplementary Fig. S5H and S5I).

Preliminary clinical activity of BETi ZEN-3694 in patients with t-NEPC

We recently completed a first-in-man, phase I trial of ZEN-3694 in combination with enzalutamide in men with metastatic CRPC progressing on enzalutamide or abiraterone (NCT02711956). Importantly, we determined that patients with the poorest response to enzalutamide or abiraterone prior to enrolling on this clinical trial or those with the lowest AR transcriptional activity in baseline biopsies experienced the best tumor control with ZEN-3694 (40). In examining the 13 baseline metastatic tissue biopsies taken prior to treatment that had tumor tissue present, we identified four subjects whose tumors had evidence of t-NEPC histology or gene expression based on activation of a previously described t-NEPC gene set (ref. 20; Supplementary Fig. S6; gene set shown in Supplementary Table S6). We confirmed this gene set was activated in t-NEPC tumors versus adenocarcinoma tumors from the Beltran dataset (ref. 21; Supplementary Fig. S6), demonstrating this signature's accuracy in identifying tumors with t-NEPC gene expression. Two of the four subjects with t-NEPC (patients 1 and 2) had prolonged disease control with ZEN-3694 (168 weeks and 40 weeks), while two other subjects (patients 3 and 4) progressed more rapidly (16 weeks and 8.5 weeks; Fig. 6A). This prolonged disease control was not explained by differences in ZEN-3694 dosage as patients 1, 2, and 3 each received 48 mg, while patient 4 received 96 mg.

Next, we examined expression of *E2F1*, *BRD4*, and *AR* in these four tumors. Tumors from the two patients with t-NEPC with prolonged disease control demonstrated higher *E2F1* and *BRD4* mRNA expression but much lower *AR* expression (Fig. 6B). Finally, the 76-gene, AR-repressed program (Supplementary Table S2) was activated in the patients with more durable control, strongly suggesting these t-NEPC tumors were more E2F1- and BRD4-dependent but less AR-dependent (Fig. 6C). These preliminary clinical results support the potential of

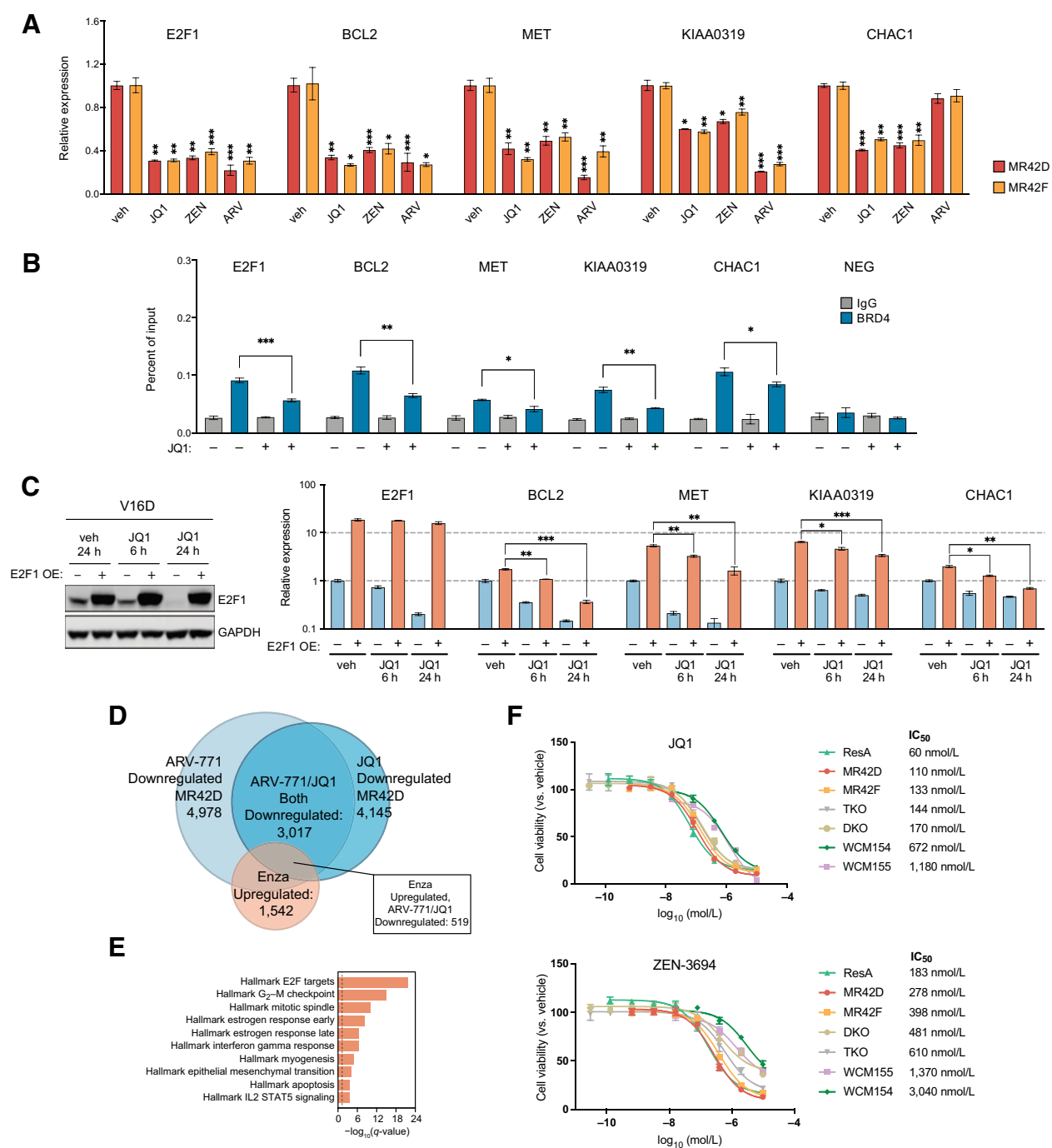


Figure 5. BET bromodomain inhibition blocks E2F1 function, t-NEPC lineage plasticity gene expression, and t-NEPC cell survival. **A**, RT-qPCR of t-NEPC genes in MR42D or MR42F cells treated with 500 nmol/L JQ1, 1 μmol/L ZEN-3694, or 5 nmol/L ARV-771 for 24 hours (*n* = 3). **B**, BRD4 ChIP-qPCR at t-NEPC gene promoters in MR42D cells treated with veh (-) or JQ1 (+) for 24 hours. Negative (NEG) control region was UNTR4 (*n* = 3). **C**, Twenty-four hours after transfection with EV (-) or E2F1 (+), V16D cells were treated with veh or 500 nmol/L JQ1 for 6 or 24 hours. Western blot of E2F1 (left). Corresponding RT-qPCR of t-NEPC genes (*n* = 3; right). **D**, Venn diagram of MR42D downregulated DEGs with ARV-771 and JQ1 versus upregulated DEGs with enzalutamide treatment with 519 overlapping genes between BETI versus enzalutamide. **E**, Top 10 enriched Hallmark categories for the 519 genes from **D** as determined by the MSigDB enrichment tool (see Methods). Dashed line corresponds to *q* = 0.05. **F**, Dose response viability curves of ResA, DKO, TKO, WCM154, WCM155, MR42D, or MR42F treated with the indicated BETI measured by CTG (*n* = 3). Calculated IC₅₀s are shown (right). DKO, TKO, WCM154, and WCM155 were treated for 72 hours, and ResA, MR42D, and MR42F were treated for 144 hours. In **A-C**, data are the average ± SD, and two-tailed Student *t* tests were performed (*, *P* < 0.05; **, *P* < 0.01; ***, *P* < 0.001).

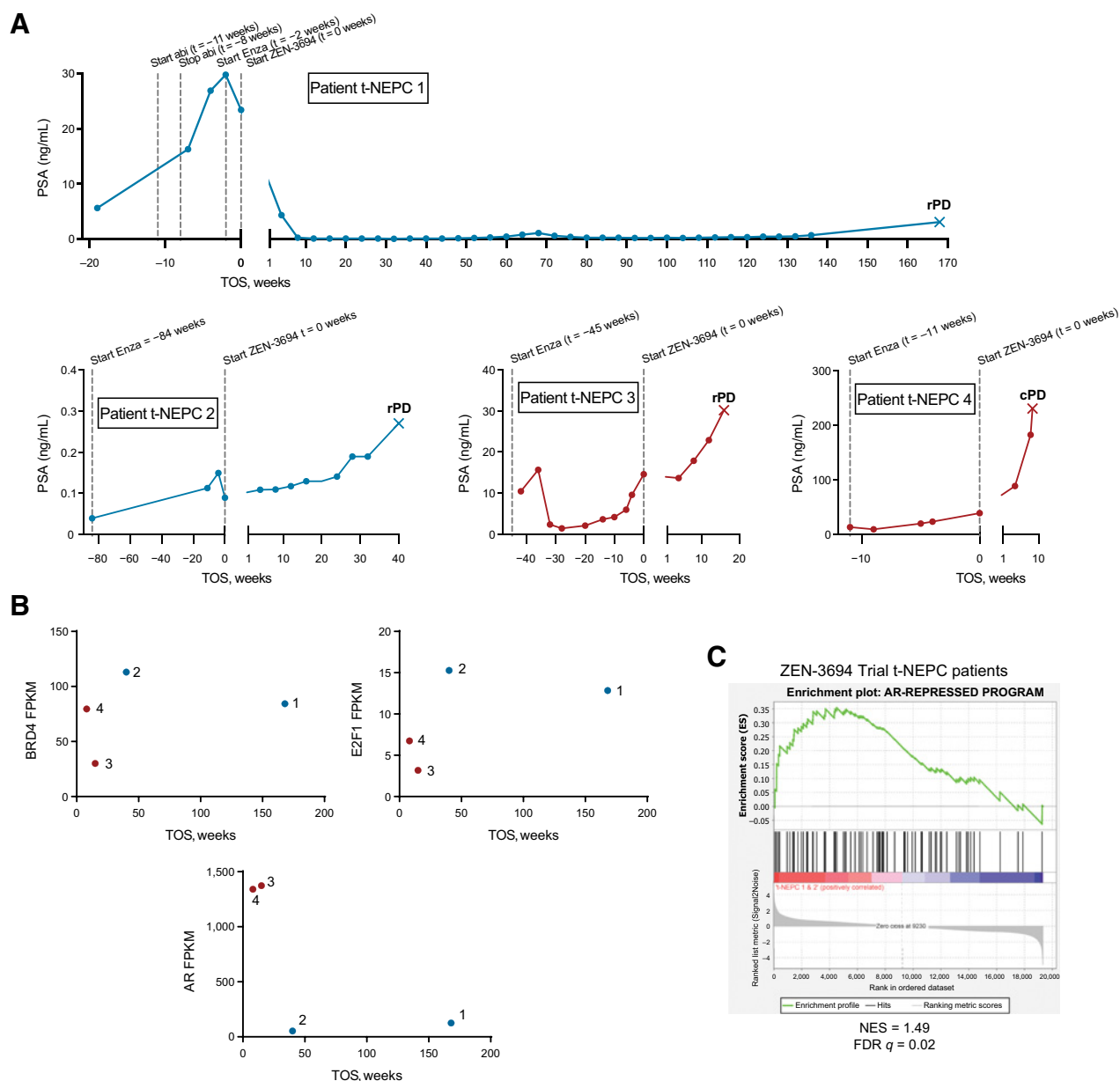


Figure 6. Preliminary clinical activity of BETi ZEN-3694 in patients with t-NEPC. **A**, Serum PSA versus time on study (TOS) profiles for the patients with t-NEPC with longer time on study (Patients t-NEPC 1 and 2) versus those with shorter time on study (Patients t-NEPC 3 and 4) on the ZEN-3694/enzalutamide clinical trial. t-NEPC patients 1, 2, and 3 were treated with 48 mg daily of ZEN-3694 + 160 mg daily of enzalutamide. t-NEPC patient 4 was treated with 96 mg daily of ZEN-3694 + 160 mg daily of enzalutamide. cPD, clinical progression of disease; rPD, radiographic progression of disease. **B**, *BRD4*, *E2F1*, and *AR* FPKM values from RNA-seq of pretreatment biopsies versus TOS for the four patients with t-NEPC shown in **A**. **C**, GSEA enrichment plot of the 76-gene, AR-repressed program shown in Supplementary Table S2 using RNA-seq data from the four t-NEPC patient tumors in the ZEN-3694 trial (tumors from t-NEPC patients 1 and 2 versus tumors from t-NEPC patients 3 and 4).

BETi to block growth of t-NEPC tumors that harbor an AR-repressed, E2F1/BRD4-activated t-NEPC lineage plasticity program.

Discussion

We previously determined that 17% of metastatic CRPC tumor biopsies have evidence of t-NEPC lineage plasticity (20). t-NEPC tumors have distinct histologic and transcriptomic profiles from adenocarcinoma tumors, and emerging data suggest that t-NEPC

tumors may develop from adenocarcinoma tumors through the acquisition of genomic and epigenomic changes induced by treatments that block AR function (21, 28, 41). Our results herein demonstrate that AR inhibition in susceptible cells activates a lineage plasticity cell survival program linked to t-NEPC and that this program may be activated through E2F1- and BRD4-dependent mechanisms.

It is well appreciated that genes activated by the AR are lost in t-NEPC tumors while neuronal gene expression is activated (21, 28). Historically, the only cell-based model used to study NEPC was the

de novo NEPC cell line NCI-H660 that lacked AR expression (42). Recent work also demonstrates that specific genomic alterations, including *PTEN*, *TP53*, and *RBI* loss, promote lineage plasticity and differentiation to nonluminal lineages and that this occurs in the setting of AR suppression and E2F1 activation in the case of *RBI* loss (26, 43). Nonetheless, the contribution of AR loss itself to lineage plasticity was still unclear, and the identity of key factors that promote activation of a t-NEPC lineage plasticity program—including factors that might normally be repressed by the AR—were poorly characterized.

We now know that loss of AR function in CRPC is a continuum and that not all tumors with loss of AR function are t-NEPC. Indeed, our own work demonstrates that there is a subset of AR-expressing, enzalutamide and abiraterone-naïve CRPC adenocarcinoma tumors that harbor an AR activity-low, stemness-high program; these tumors are much less likely to respond to enzalutamide treatment (16). Furthermore, some AR activity-low tumors—so-called double negative prostate cancer (tumors negative for both AR and NEPC markers)—lose AR expression without NEPC differentiation, and these tumors appear to be increasing in frequency (44, 45). This demonstrates that AR loss is not sufficient for t-NEPC development.

A subset of enzalutamide- and abiraterone-resistant tumors demonstrates t-NEPC lineage plasticity; AR function is suppressed in these t-NEPC tumors even though some continue to express the AR (16, 20, 45). Our results suggest that treatment with AR inhibitors may block AR function and contribute to activation of a t-NEPC lineage plasticity program or that AR inhibitors select for preexisting clones with this phenotype in patients. Indeed, we showed that pharmacologic AR inhibition in cell models and patient tumors activates an AR-repressed program that promotes t-NEPC lineage plasticity. Moreover, using AR activity-low or t-NEPC lineage plasticity tumor models (25, 26), we confirmed that AR loss of function or expression coincides with activation of an AR-repressed, lineage plasticity program, highlighting the clinical relevance of the program we identified and the cell systems we used. Furthermore, these results suggest that persistent loss of AR function or expression may lock in this lineage plasticity program in certain tumors, potentially making them more reliant on critical factors that maintain this program.

Importantly, several of the AR-repressed genes in the program we identified have been shown previously to promote survival of t-NEPC tumors or AR activity-low tumors, including *MET* and *BCL2*, and are targetable with drugs approved for other cancers (29, 30, 46). This suggests that these drugs are worthy of further study in t-NEPC and other AR activity-low tumors. Indeed, a clinical trial with the *BCL2* inhibitor venetoclax is ongoing in men with CRPC (NCT03751436).

The chromatin landscape of cells is critical for the regulation of gene expression, and this landscape varies widely across tissue types, including in cancer (47, 48). Importantly, our ATAC-seq studies demonstrate that enzalutamide-resistant t-NEPC cells have a distinct chromatin accessibility profile versus adenocarcinoma cells and that the top hyper-accessible chromatin regions in t-NEPC are linked with neuronal differentiation as opposed to metabolic processes. While it is unclear what mechanisms explain the greater chromatin accessibility profiles for neuronal genes between these cell types, these changes appear to have been induced during the acquisition of enzalutamide resistance. Our results suggest that the chromatin context in which AR is suppressed may be an important determinant of which specific genes are activated and the phenotype that ensues. Further study is clearly warranted to understand whether specific differences in chromatin hyper-accessibility—like those we observed—are linked with t-NEPC or the risk of t-NEPC's emergence after treatment with AR inhibitors.

Significantly, we demonstrated that the master regulator transcription factor E2F1 may be a key player that promotes t-NEPC lineage plasticity through activation of genes normally repressed by the AR. Indeed, E2F1 overexpression in adenocarcinoma cells was sufficient to activate expression of genes highly expressed in t-NEPC, and E2F1 overexpression coincided with E2F1, H3K27ac, and BRD4 cooccupancy on chromatin, suggesting E2F1 may promote chromatin changes that facilitate NEPC lineage plasticity. Furthermore, E2F1 overexpression blunted the growth-suppressive effects of enzalutamide, indicating that E2F1 may confer enzalutamide resistance. Taken together, these data strongly suggest E2F1 is a factor worthy of further study in t-NEPC.

Although E2F1 is not currently targetable, we determined that BETi blocks E2F1 activation of t-NEPC gene expression, demonstrating cooperativity between E2F1 and BET bromodomain proteins. While our studies focused on E2F1, we fully acknowledge that other transcription factors are important for activation of this t-NEPC program and that mechanisms described herein may be recapitulated by other master regulators. Indeed, because of the redundancy of transcription factors for promoting phenotypes such as t-NEPC, we predict an approach to target them broadly through shared cooperating factors—such as BET bromodomain proteins—would be more effective than targeting any single transcription factor.

The antitumor activity of BETi in CRPC has been primarily linked to suppression of AR function (37, 49). However, we recently demonstrated that BETi also blocks the growth of AR-null adenocarcinoma CRPC tumors in preclinical studies (34, 38) and growth of patient tumors that responded poorly to enzalutamide or abiraterone, many of which are AR activity-low (40). Thus, though this current report focuses on t-NEPC, it is clear that mechanisms of BETi response described herein may also be quite relevant to AR activity-low tumors that may not have undergone t-NEPC lineage plasticity.

Importantly, we also determined that BETi treatment blocks expression of AR-repressed genes highly expressed in t-NEPC tumors, strongly suggesting that BET bromodomain proteins are critically important for promoting adaptive survival in t-NEPC tumors with loss of AR function. BETi suppressed growth of t-NEPC cell lines and patient-derived organoids and induced death of patient-derived xenograft cultures. Finally, treatment with the BETi ZEN-3694 led to prolonged tumor control in patients with t-NEPC whose tumors harbored high *E2F1* and *BRD4* expression and activation of the 76-gene, AR-repressed gene program we identified. These early clinical results suggest the potential of BETi in a subset of men whose tumors have undergone t-NEPC lineage plasticity—patients for whom there are currently no effective treatment options.

The significance of t-NEPC lineage plasticity as a critical determinant of resistance to AR-signaling inhibitors is becoming increasingly evident (19, 20). We anticipate that future studies will identify additional therapeutic vulnerabilities—like E2F1 and BRD4 cooperativity—that will lead to the design of rational clinical trials to more effectively control subsets of tumors that have undergone t-NEPC lineage plasticity.

Authors' Disclosures

H. Beltran reports grants and other support from Janssen; grants from Abbvie and Bristol Myers Squibb; and other support from Amgen, Pfizer, Foundation Medicine, Blue Earth, Sanofi Genzyme, Merck, and AstraZeneca outside the submitted work. P.S. Nelson reports personal fees from Janssen, Bristol Myers Squibb, and Astellas outside the submitted work. E. Corey reports grants from NIH during the conduct of the study, as well as other support from AbbVie, Janssen Research and Development, Genentech, Forma Therapeutics, Kronos Bio, Bayer, GSK, Arvinas, AstraZeneca, and Sanofi outside the submitted work. R. Aggarwal reports grants and personal fees from

AstraZeneca, personal fees from Dendreon, and grants from Janssen, Amgen, Merck, and Zenith Epigenetics outside the submitted work. W. Abida reports other support from Zenith Epigenetics during the conduct of the study. W. Abida also reports personal fees and other support from Clovis Oncology, ORIC Pharmaceuticals, and GSK; personal fees from Janssen, MORE Health, and Daiichi Sankyo; and other support from AstraZeneca, Epizyme, Medscape, Roche, and Aptitude Health outside the submitted work. F.Y. Feng reports personal fees from Janssen, Blue Earth Diagnostics, Astellas, Myovant, Roivant, Bayer, Celgene, SerImmune, Bristol Myers Squibb, Exact Sciences, Varian, and Foundation Medicine outside the submitted work. E.J. Small reports non-financial support from Harpoon Therapeutics, as well as personal fees from Fortis Therapeutics, Janssen, Johnson and Johnson, Teon Therapeutics, Ultragenyx, BeiGene, and Tolero outside the submitted work. D.E. Spratt reports grants and personal fees from Janssen, as well as personal fees from Blue Earth, AstraZeneca, and Boston Scientific outside the submitted work. A. Rao reports grants from NIH, ACS, and Agilent Technologies; other support from Voxal Analytics, LLC, Genophyll, LLC, and Texas A&M IBT; and institutional funds from University of Michigan Ann Arbor during the conduct of the study. A. Rao also reports other support from CHI outside the submitted work, and is member of Voxal Analytics, LLC. E.M. Gesner reports other support from Zenith Epigenetics Ltd. during the conduct of the study, as well as other support from Zenith Epigenetics Ltd. outside the submitted work. S. Attwell reports other support from Zenith Epigenetics Ltd. during the conduct of the study, as well as other support from Zenith Epigenetics Ltd. outside the submitted work; in addition, S. Attwell has a patent for Combination Therapy for the Treatment of Prostate Cancer issued to Zenith Epigenetics Ltd. S. Lakhota reports other support from Zenith Epigenetics during the conduct of the study, as well as other support from Zenith Epigenetics outside the submitted work. E. Campeau reports other support from Zenith Epigenetics Ltd. during the conduct of the study, as well as other support from Zenith Epigenetics Ltd. outside the submitted work; in addition, E. Campeau has a patent for Combination Therapy for the Treatment of Prostate Cancer issued to Zenith Epigenetics Ltd. J.J. Alumkal reports other support from Zenith Epigenetics, personal fees from Astellas, and grants from NCI, Department of Defense, Kuni Foundation, and Sheppard Family Fund during the conduct of the study. J.J. Alumkal also reports personal fees from Janssen Biotech, Merck Sharp & Dohme, and Dendreon outside the submitted work. No disclosures were reported by the other authors.

Disclaimer

The content is solely the responsibility of the authors and does not necessarily represent the official views of the NIH or DoD.

Authors' Contributions

D.-H. Kim: Formal analysis, validation, investigation, writing–review and editing. **D. Sun:** Data curation, formal analysis, investigation, visualization, writing–original draft, writing–review and editing. **W.K. Storck:** Formal analysis, validation, investigation, visualization, writing–original draft, writing–review and editing. **K. Welker Leng:** data curation, formal analysis, writing–review and editing. **C. Jenkins:** Formal analysis, validation, investigation, writing–original draft, writing–review and editing. **D.J. Coleman:** Formal analysis, validation, investigation, writing–review and editing. **D. Sampson:** Validation, investigation, writing–review

and editing. **X. Guan:** Data curation, formal analysis, writing–review and editing. **A. Kumaraswamy:** Formal analysis, validation, investigation, visualization, writing–review and editing. **E.S. Rodansky:** Validation, investigation, writing–review and editing. **J.A. Urrutia:** Formal analysis, validation, investigation, writing–review and editing. **J.A. Schwartzman:** Formal analysis, validation, investigation, writing–review and editing. **C. Zhang:** Validation, investigation, writing–review and editing. **H. Beltran:** Resources, formal analysis, validation, investigation, writing–review and editing. **M.P. Labrecque:** Formal analysis, validation, investigation, writing–review and editing. **C. Morrissey:** Formal analysis, validation, investigation, writing–review and editing. **J.M. Lucas:** Formal analysis, validation, investigation, writing–review and editing. **I.M. Coleman:** Formal analysis, writing–review and editing. **P.S. Nelson:** Formal analysis, writing–review and editing. **E. Corey:** Resources, writing–review and editing. **S.K. Handelman:** Formal analysis, writing–review and editing. **J.Z. Sexton:** Formal analysis, writing–review and editing. **R. Aggarwal:** Resources, formal analysis, validation, investigation, writing–review and editing. **W. Abida:** Validation, investigation, writing–review and editing. **F.Y. Feng:** Formal analysis, writing–review and editing. **E.J. Small:** Formal analysis, writing–review and editing. **D.E. Spratt:** Formal analysis, writing–review and editing. **A. Bankhead III:** Data curation, formal analysis, writing–review and editing. **A. Rao:** Formal analysis, writing–review and editing. **E.M. Gesner:** Formal analysis, writing–review and editing. **S. Attwell:** Formal analysis, validation, investigation, writing–review and editing. **S. Lakhota:** Validation, investigation, writing–review and editing. **E. Campeau:** Formal analysis, validation, investigation, writing–review and editing. **J.A. Yates:** Formal analysis, supervision, validation, investigation, visualization, writing–original draft, project administration, writing–review and editing. **Z. Xia:** Formal analysis, supervision, writing–original draft, writing–review and editing. **J.J. Alumkal:** Conceptualization, formal analysis, supervision, funding acquisition, investigation, visualization, methodology, writing–original draft, project administration, writing–review and editing.

Acknowledgments

This work was supported by NCI R01 CA251245, R01CA234715, the NCI Pacific Northwest Prostate Cancer SPORE (P50 CA097186), the NCI Michigan Prostate SPORE (P50 CA186786), the NCI Drug Resistance and Sensitivity Network (P50 CA186786–07S1, U54CA224079), Department of Defense Impact Award W81XWH-16-1-0597, and Department of Defense Prostate Cancer Research Program Physician Research Award (W81XWH-17-1-0124). Other support includes Prostate Cancer Foundation Young Investigator Award, Kuni Foundation, a University of Michigan Rogel Scholar Award and Rogel Innovation Award/NCI P30 CA046592, and a Sheppard Family Fund Sheppard Scholar Award. OHSU, UCSF, and MSKCC received research funding from Zenith Epigenetics to conduct the industry-sponsored ZEN-3694 clinical trial.

The costs of publication of this article were defrayed in part by the payment of page charges. This article must therefore be hereby marked *advertisement* in accordance with 18 U.S.C. Section 1734 solely to indicate this fact.

Received December 24, 2020; revised April 15, 2021; accepted June 15, 2021; published first June 18, 2021.

References

- Montgomery RB, Mostaghel EA, Vessella R, Hess DL, Kalthorn TF, Higano CS, et al. Maintenance of intratumoral androgens in metastatic prostate cancer: a mechanism for castration-resistant tumor growth. *Cancer Res* 2008;68:4447–54.
- Smith MR, Saad F, Chowdhury S, Oudard S, Hadaschik BA, Graff JN, et al. Apalutamide treatment and metastasis-free survival in prostate cancer. *N Engl J Med* 2018;378:1408–18.
- Scher HI, Beer TM, Higano CS, Anand A, Taplin ME, Efstathiou E, et al. Antitumor activity of MDV3100 in castration-resistant prostate cancer: a phase 1–2 study. *Lancet* 2010;375:1437–46.
- Beer TM, Armstrong AJ, Rathkopf DE, Loriot Y, Sternberg CN, Higano CS, et al. Enzalutamide in metastatic prostate cancer before chemotherapy. *N Engl J Med* 2014;371:424–33.
- Ryan CJ, Smith MR, de Bono JS, Molina A, Logothetis CJ, de Souza P, et al. Abiraterone in metastatic prostate cancer without previous chemotherapy. *N Engl J Med* 2013;368:138–48.
- Fizazi K, Shore N, Tammela TL, Ulys A, Vjaters E, Polyakov S, et al. Darolutamide in nonmetastatic, castration-resistant prostate cancer. *N Engl J Med* 2019;380:1235–46.
- Armstrong AJ, Szmulewitz RZ, Petrylak DP, Holzbeierlein J, Villers A, Azad A, et al. ARCHES: a randomized, phase III study of androgen deprivation therapy with enzalutamide or placebo in men with metastatic hormone-sensitive prostate cancer. *J Clin Oncol* 2019;37:2974–86.
- Chi KN, Agarwal N, Bjartell A, Chung BH, Pereira de Santana Gomes AJ, Given R, et al. Apalutamide for metastatic, castration-sensitive prostate cancer. *N Engl J Med* 2019;381:13–24.
- Davis ID, Martin AJ, Stockler MR, Begbie S, Chi KN, Chowdhury S, et al. Enzalutamide with standard first-line therapy in metastatic prostate cancer. *N Engl J Med* 2019;381:121–31.
- Fizazi K, Tran N, Fein L, Matsubara N, Rodriguez-Antolin A, Alekseev BY, et al. Abiraterone plus prednisone in metastatic, castration-sensitive prostate cancer. *N Engl J Med* 2017;377:352–60.

11. Antonarakis ES, Lu C, Wang H, Luber B, Nakazawa M, Roeser JC, et al. AR-V7 and resistance to enzalutamide and abiraterone in prostate cancer. *N Engl J Med* 2014;371:1028–38.
12. Quigley DA, Dang HX, Zhao SG, Lloyd P, Aggarwal R, Alumkal JJ, et al. Genomic hallmarks and structural variation in metastatic prostate cancer. *Cell* 2018;174:758–69.
13. Robinson D, Van Allen EM, Wu YM, Schultz N, Lonigro RJ, Mosquera JM, et al. Integrative clinical genomics of advanced prostate cancer. *Cell* 2015;161:1215–28.
14. Takeda DY, Spisak S, Seo JH, Bell C, O'Connor E, Korthauer K, et al. A somatically acquired enhancer of the androgen receptor is a noncoding driver in advanced prostate cancer. *Cell* 2018;174:422–32.
15. Asangani I, Blair IA, Van Duyne G, Hilser VJ, Moiseenkova-Bell V, Plymate S, et al. Using biochemistry & biophysics to extinguish androgen receptor signaling in prostate cancer. *J Biol Chem* 2021;296:100240.
16. Alumkal JJ, Sun D, Lu E, Beer TM, Thomas GV, Latour E, et al. Transcriptional profiling identifies an androgen receptor activity-low, stemness program associated with enzalutamide resistance. *Proc Natl Acad Sci U S A* 2020;117:12315–23.
17. Zhang D, Park D, Zhong Y, Lu Y, Rycak K, Gong S, et al. Stem cell and neurogenic gene-expression profiles link prostate basal cells to aggressive prostate cancer. *Nat Commun* 2016;7:10798.
18. Spratt DE, Alshalalfa M, Fishbane N, Weiner AB, Mehra R, Mahal BA, et al. Transcriptomic heterogeneity of androgen receptor activity defines a de novo low AR-active subclass in treatment naive primary prostate cancer. *Clin Cancer Res* 2019;25:6721–30.
19. Beltran H, Hruszkewycz A, Scher HI, Hildesheim J, Isaacs J, Yu EY, et al. The role of lineage plasticity in prostate cancer therapy resistance. *Clin Cancer Res* 2019;25:6916–24.
20. Aggarwal R, Huang J, Alumkal JJ, Zhang L, Feng FY, Thomas GV, et al. Clinical and genomic characterization of treatment-emergent small-cell neuroendocrine prostate cancer: a multi-institutional prospective study. *J Clin Oncol* 2018;36:2492–503.
21. Beltran H, Prandi D, Mosquera JM, Benelli M, Puca L, Cyrta J, et al. Divergent clonal evolution of castration-resistant neuroendocrine prostate cancer. *Nat Med* 2016;22:298–305.
22. Humphrey PA. Histological variants of prostatic carcinoma and their significance. *Histopathology* 2012;60:59–74.
23. Smith BA, Sokolov A, Uzunangelov V, Baertsch R, Newton Y, Graim K, et al. A basal stem cell signature identifies aggressive prostate cancer phenotypes. *Proc Natl Acad Sci U S A* 2015;112:E6544–E52.
24. Bishop JL, Thaper D, Vahid S, Davies A, Ketola K, Kuruma H, et al. The master neural transcription factor BRN2 is an androgen receptor-suppressed driver of neuroendocrine differentiation in prostate cancer. *Cancer Discov* 2017;7:54–71.
25. Handle F, Prekovic S, Helsen C, Van den Broeck T, Smeets E, Moris L, et al. Drivers of AR indifferent anti-androgen resistance in prostate cancer cells. *Sci Rep* 2019;9:13786.
26. Ku SY, Rosario S, Wang Y, Mu P, Seshadri M, Goodrich ZW, et al. Rb1 and Trp53 cooperate to suppress prostate cancer lineage plasticity, metastasis, and anti-androgen resistance. *Science* 2017;355:78–83.
27. Haram KM, Peltier HJ, Lu B, Bhasin M, Otu HH, Choy B, et al. Gene expression profile of mouse prostate tumors reveals dysregulations in major biological processes and identifies potential murine targets for preclinical development of human prostate cancer therapy. *Prostate* 2008;68:1517–30.
28. Aggarwal RR, Quigley DA, Huang J, Zhang L, Beer TM, Rettig MB, et al. Whole genome and transcriptional analysis of treatment-emergent small cell neuroendocrine prostate cancer demonstrates intra-class heterogeneity. *Mol Cancer Res* 2019;17:1235–40.
29. Qiao Y, Feng FY, Wang Y, Cao X, Han S, Wilder-Romans K, et al. Mechanistic support for combined MET and AR blockade in castration-resistant prostate cancer. *Neoplasia* 2016;18:1–9.
30. Li Q, Deng Q, Chao HP, Liu X, Lu Y, Lin K, et al. Linking prostate cancer cell AR heterogeneity to distinct castration and enzalutamide responses. *Nat Commun* 2018;9:1–17.
31. Dali R, Verginelli F, Pramatarova A, Sladek R, Stifani S. Characterization of a FOXG1:TLE1 transcriptional network in glioblastoma-initiating cells. *Mol Oncol* 2018;12:775–87.
32. Franquinho F, Nogueira-Rodrigues J, Duarte JM, Esteves SS, Carter-Su C, Monaco AP, et al. The dyslexia-susceptibility protein KIAA0319 inhibits axon growth through Smad2 signaling. *Cereb Cortex* 2017;27:1732–47.
33. Roe JS, Mercan F, Rivera K, Pappin DJ, Vakoc CR. BET bromodomain inhibition suppresses the function of hematopoietic transcription factors in acute myeloid leukemia. *Mol Cell* 2015;58:1028–39.
34. Coleman DJ, Gao L, King CJ, Schwartzman J, Urrutia J, Sehrawat A, et al. BET bromodomain inhibition blocks the function of a critical AR-independent master regulator network in lethal prostate cancer. *Oncogene* 2019;38:5658–69.
35. Alvarez MJ, Giorgi F, Califano A. Using viper, a package for virtual inference of protein-activity by enriched regulon analysis. *Bioconductor* 2014:1–14.
36. Julian LM, Blais A. Transcriptional control of stem cell fate by E2Fs and pocket proteins. *Front Genet* 2015;6:1–15.
37. Asangani IA, Dommeti VL, Wang X, Malik R, Cieslik M, Yang R, et al. Therapeutic targeting of BET bromodomain proteins in castration-resistant prostate cancer. *Nature* 2014;510:278–82.
38. Coleman DJ, Gao L, Schwartzman J, Korkola JE, Sampson D, Derrick DS, et al. Maintenance of MYC expression promotes de novo resistance to BET bromodomain inhibition in castration-resistant prostate cancer. *Sci Rep* 2019;9:1–9.
39. Puca L, Bareja R, Prandi D, Shaw R, Benelli M, Karthaus WR, et al. Patient derived organoids to model rare prostate cancer phenotypes. *Nat Commun* 2018;9:1–10.
40. Aggarwal RR, Schweizer MT, Nanus DM, Pantuck AJ, Heath EI, Campeau E, et al. A phase Ib/IIa study of the pan-BET inhibitor ZEN-3694 in combination with enzalutamide in patients with metastatic castration-resistant prostate cancer. *Clin Cancer Res* 2020;26:5338–47.
41. Zou M, Toivanen R, Mitrofanova A, Floch N, Hayati S, Sun Y, et al. Transdifferentiation as a mechanism of treatment resistance in a mouse model of castration-resistant prostate cancer. *Cancer Discov* 2017;7:736–49.
42. Carney DN, Gazdar AF, Bepler G, Guccion JG, Marangos PJ, Moody TW, et al. Establishment and identification of small cell lung cancer cell lines having classic and variant features. *Cancer Res* 1985;45:2913–23.
43. Mu P, Zhang Z, Benelli M, Karthaus WR, Hoover E, Chen CC, et al. SOX2 promotes lineage plasticity and antiandrogen resistance in TP53- and RB1-deficient prostate cancer. *Science* 2017;355:84–8.
44. Cackowski FC, Kumar-Sinha C, Mehra R, Wu YM, Robinson DR, Alumkal JJ, et al. Double-negative prostate cancer masquerading as a squamous cancer of unknown primary: a clinicopathologic and genomic sequencing-based case study. *JCO Precis Oncol* 2020;4:PO.20.00309.
45. Labrecque MP, Coleman IM, Brown LG, True LD, Kollath L, Lakely B, et al. Molecular profiling stratifies diverse phenotypes of treatment-refractory metastatic castration-resistant prostate cancer. *J Clin Invest* 2019;130:4492–505.
46. Liang Y, Jeganathan S, Marastoni S, Sharp A, Figueiredo I, Marcellus R, et al. Emergence of enzalutamide resistance in prostate cancer is associated with BCL-2 and IKK β dependencies. *Clin Cancer Res* 2021;27:2340–51.
47. Corces MR, Granja JM, Shams S, Louie BH, Seoane JA, Zhou W, et al. The chromatin accessibility landscape of primary human cancers. *Science* 2018;362:1–13.
48. Pomerantz MM, Qiu X, Zhu Y, Takeda DY, Pan W, Baca SC, et al. Prostate cancer reactivates developmental epigenomic programs during metastatic progression. *Nat Genet* 2020;52:790–9.
49. Faivre EJ, McDaniel KF, Albert DH, Mantena SR, Plotnik JP, Wilcox D, et al. Selective inhibition of the BD2 bromodomain of BET proteins in prostate cancer. *Nature* 2020;578:306–10.